

Enhancing Quality of Pose-varied Face Restoration with Local Weak Feature Sensing and GAN Prior

Kai Hu, *Student Member, IEEE*, Yu Liu, Renhe Liu, Wei Lu* Gang Yu, Bin Fu

Abstract—Facial semantic guidance (facial landmarks, facial parsing maps, facial heatmaps, etc.) and facial generative adversarial networks (GAN) prior have been widely used in blind face restoration (BFR) in recent years. Although existing BFR methods have achieved good performance in ordinary cases, these solutions have limited resilience when applied to face images with serious degradation and pose-varied (look up, look down, laugh, etc.) in real-world scenarios. In this work, we propose a well-designed blind face restoration network with generative facial prior. The proposed network is mainly comprised of an asymmetric codec and StyleGAN2 prior network. In the asymmetric codec, we adopt a mixed multi-path residual block (MMRB) to gradually extract weak texture features of input images, which can improve the texture integrity and authenticity of our networks. Furthermore, the MMRB block can also be plug-and-play in any other network. Besides, a novel self-supervised training strategy is specially designed for face restoration tasks to fit the distribution closer to the target and maintain training stability. Extensive experiments over synthetic and real-world datasets demonstrate that our model achieves superior performance to the prior art for face restoration and face super-resolution tasks and can tackle seriously degraded face images in diverse poses and expressions.

Index Terms—Blind Face Restoration, StyleGAN2, Asymmetric Codec, Self-supervised Training.

I. INTRODUCTION

BLIND Face restoration (BFR) is typically an ill-posed image inverse problem and aims at reproducing real and reasonable high-quality face images from unknown degraded inputs. In the wild, face images often suffer from the joint action of multiple unknown degradation factors, such as low resolution, noise, blur [1], compression artifacts [2], etc., resulting in the serious loss of detailed information in the image and affecting the overall image quality. In particular, due to the complex and diverse degradation factors, no-single facial posture, and a large range of motion, multi-pose face images are generally difficult to restore the real and natural results and are still a challenge for BFR tasks.

As a highly structured object, the human face has some specific characteristics. Previous works based on CNN and GAN use various facial semantic priors (including facial landmarks [25], [26], [62], facial parsing maps [1], [5], [13], [22],

Manuscript received xx; revised xx. This work was supported in part by xx Kai Hu, Yu Liu, and Renhe Liu are with the School of Microelectronics, Tianjin University, Tianjin 300110, China (e-mail: xxx). Wei Lu is with the School of Electrical and Information, Tianjin University, Tianjin 300110, China (e-mail: xxx).

Gang Yu and Bin Fu are with Applied Research Center (ARC), Tencent PCCG.

Copyright © 2022 IEEE. Personal use of this material is permitted. However, permission to use this material for any other purposes must be obtained from the IEEE by sending an email to pubs-permissions@ieee.org.



Fig. 1. Restoration results from the old photos of the Solvay conference, 1927. And display some face images. Please zoom in for the best view.

facial heatmaps [4], and facial component dictionaries [7]) to guide the networks to recover face shape and details. However, when used to restore seriously degraded images, there is limited prior information, and the facial structure in the restored images can be improved.

Thanks to the proposal of generative facial models, such as StyleGAN [19], StyleGAN2 [20], and StyleGAN3 [21], they are capable of synthesizing face images with rich textures, changeable styles, and highly realistic vision, and provide rich and diverse priors such as facial contours and textures of all areas (including hair, eyes, and teeth). So far, StyleGAN2 has been widely used for face restoration tasks, such as PULSE [11], pSp [13], PSFR-GAN [5], GFPGAN [15], GPEN [16], GCFSR [6], and Panini-Net [17]. Although these methods have fully used the StyleGAN2 network or the pre-trained prior model, they are still much room for improvement in the restoration results. This is mainly due to the lack of appropriate and efficient training strategies for the GAN prior.

All in all, when used to solve the seriously degraded pose-varied face image, the existing methods often have problems such as excessive fantasy or blur, artifact, and unreasonable texture. To address this challenging problem, we propose a novel blind face restoration network with the GAN prior [20], composed of an asymmetric codec and StyleGAN2 prior network. Firstly, since there are few weak texture features in degraded images, we propose a mixed multi-path residual block (MMRB), which can equally split the input features and make use of different convolution kernels to extract and fuse the features fully. The MMRB layer therefore can reduce the number of parameters introduced by the network and improve the overall performance of our model.

Secondly, To better restore natural and high-quality (HQ) face images, as shown in Fig. 1, we use StyleGAN2 with

generative facial prior as the primary generator network and jointly fine-tune the generator with the codec. Using facial landmark points of training data, the position coordinates of the local areas are obtained, such as the eyes and mouth. Then we adopt local facial losses to improve the authenticity of the output facial results during training. Finally, we introduce a training strategy of freezing a pre-trained discriminator (FreezeD), which helps our network recover more reasonable and high fidelity results in complex degraded scenes. In particular, this training strategy helps our model to remain stable during training and speed up the fitting of the generated results to the target distribution.

The main contributions of this work are summarized as follows:

- We propose a well-designed blind face restoration network with generative facial prior, which can be used to improve the quality of face images with complex facial posture and serious degradation.
- For the StyleGAN2 prior model, we specially design a novel self-supervised training strategy that freezes a pre-trained discriminator (FreezeD) and jointly fine-tunes the generator with the codec. It helps our model recover high-quality face images more realistically and reasonably in complex degraded scenes and maintain stability during training.
- To better extract few and weak texture features in low-quality images and avoid excessive fantasy in our model, we propose an MMRB layer, which can equally split multi-channel feature maps, adaptively extract image features by using different convolution kernels and share the features with each other.
- Extensive experiments show that our method achieves state-of-the-art results on synthetic and real-world datasets. It can observe that our restored results have a more realistic and natural facial texture and are closer to input images while avoiding the excessive fantasy of the faces.

II. RELATED WORK

A. Face Restoration

For blind face restoration(BFR) in the real world, the restoration problem becomes more complex due to the particularity of the face image itself and the influence of many unknown degradation factors, such as compression artifacts, low resolution, blur, and noise. There are three main research trends [24] for this task: basic CNN-based methods, GAN-based methods, and Prior-guided methods.

Basic CNN-based methods. Bi-channel CNN [29] introduced an end-to-end Bi-channel CNN which can adaptively integrate two channels of information to handle significant appearance variations and blur effects. DPDFN [28] proposed a simple dual-path deep fusion network for face image super-resolution without additional face prior, which constructed two individual branches for learning global facial contours and local face details and then fused the result of the two branches. SPARNet [45] proposed face attention units for face super-resolution. and introduced a spatial attention mechanism to

vanilla residual blocks to produce high-quality(HQ) and high-resolution outputs.

GAN-based methods. HiFaceGAN [12] proposed a collaborative suppression and replenishment framework to tackle unconstrained face restoration problems. TDAE [3] presented a discriminative generative network, which was not affected by posture and facial expression and can ultra-resolve low-resolution face images. SPGAN [30] designed a supervised pixel-wise GAN whose discriminator was used to output the same resolution matrix as the input image and proposed a supervised pixel-wise adversarial loss. RWSR [44] proposed a novel method to synthesize low-quality images for face super-resolution and used the ESRGAN [18] model as the main backbone SR model, which introduced a variety of loss functions to improve image quality. Super-FAN [4] first proposed an end-to-end model that addressed face super-resolution and alignment via integrating a sub-network for face alignment through heat map regression and optimizing a heatmap loss. mGANprior [10] as a GAN inversion method optimized multiple codes and adopted an adaptive channel importance strategy. It can be applied to tasks related to multiple image processing. PSFR-GAN [5] based on the StyleGAN2 network adopted a semantic-aware style transfer approach to modulate the features of different scales and recover HQ face details progressively. GCFSR [6] proposed a generative and controllable face super-resolution model without reliance on any additional priors, which can use to reconstruct faithful images with promising identity information.

GAN Prior-guided methods. The pre-trained model based on StyleGAN2 [20] is often used to solve the GAN inversion problem, such as face restoration and face super-resolution. PULSE [11] adopted a self-supervised training method to iteratively optimize the latent codes of StyleGAN2 until the distance between outputs and inputs was below a threshold to restore real facial images. pSp [13] utilized the pre-trained StyleGAN2 model and used a standard feature pyramid as an encoder network to solve image-to-image translation tasks. GFPGAN [15] also used the pre-trained StyleGAN2 model as a generative facial prior and then proposed Channel-Split Spatial Feature Transform layers to perform spatial modulation on a split of features to improve the quality of face images. GPEN [16] directly embedded GAN prior into the codec structure as the decoder and jointly fine-tuned the GAN prior network with the DNN. Panini-Net [17] proposed a learnable mask to dynamically fuse the encoder's features with the features generated by GAN blocks in the pre-trained StyleGAN2 model and adopted a contrastive learning strategy [42] to extract discriminative degradation representations for degraded images. Although high-quality face images can be restored using the GAN prior, their restoration results are not accurate enough for the images with multiple faces and serious degradation. Therefore, we introduce a self-supervised training strategy to train the codec network with the generative facial prior model jointly.

B. Transfer GAN Priors

Transfer GAN prior model is also regarded as a domain adaptation, which is the task of adapting a model to different

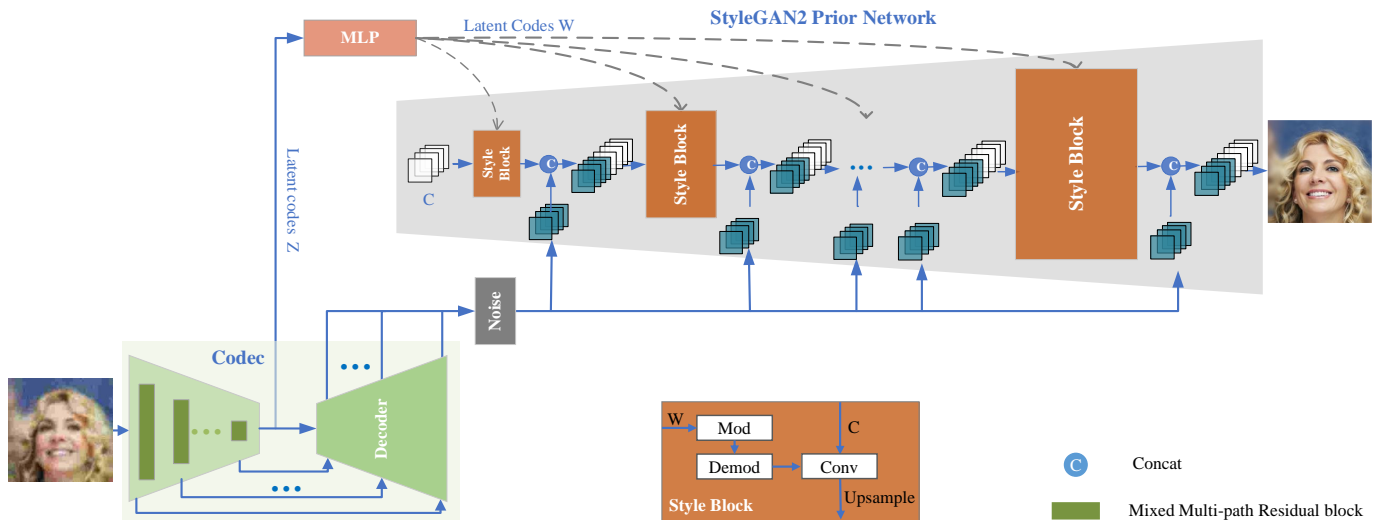


Fig. 2. The framework of our proposed method. It is mainly composed of an asymmetric codec and StyleGAN2 prior network. The MMRB layer is adopted to gradually extract weak texture features of input images in the encoder. Furthermore, the input of the GAN prior network includes latent codes W , a learned constant feature tensor C and noise branches.

domains [30], [41], [50]–[52]. For the pre-trained model, common use strategies are fine-tuning training and fixed-parameter training. However, directly using GAN Priors for training cannot reduce the difference between the two data distributions and improve the restored image quality [48]. Therefore, it needs to adopt appropriate fine-tuning training strategies, especially for seriously degraded image restoration tasks. Most relevant to our work, domain adaptation methods ([37]–[39]) build upon StyleGAN [19] [20] demonstrated impressive visual quality and semantic interpretability in the target domain. StyleGAN-ADA [52] proposed an adaptive discriminator augmentation method to train StyleGAN on limited data. Mo et al. [49] froze lower layers of the discriminator to achieve domain adaptation and demonstrated the effectiveness of this simple baseline using various architectures and datasets. Huang et al. [40] proposed an Image-to-Image translation method that generated a new model in the target domain via a series of model transformations on a pre-trained StyleGAN2 model in the source domain.

C. Feature Extraction Block

So far, various feature extraction blocks have been proposed to improve the learning ability of convolution layers in a network. Multiple versions of inception blocks [36] [57] adopted multiple-scale convolution kernels in the network to replace the dense structure, and fused all convolution results, and used the bottleneck layer for dimensionality reduction to reduce the amount of network computing. Kim et al. [35] added a short connection to the previous convolution layer and put forward the idea of residual learning, which can effectively alleviate the disappearance of gradients during training and reduce the number of parameters. After that, Zhang et al. [34] mainly increased the width of convolution by using the information compensation of other feature channels, which can reduce the vanishing gradient, realize the efficient utilization of feature information and enhance the transmission

of features. Li et al. [46] motivated by the inception module proposed a multiscale residual block to exploit the features of images at different scales. Inspired by the above methods, we propose a mixed multi-path residual block (MMRB) to extract image features of different paths and realize mixed interaction between features to provide better modeling capabilities for face restoration.

III. OUR PROPOSED METHODS

A. Global Architecture

In this section, we will describe the well-designed network framework in Fig. 2, which can be used to solve a serious ill-posed inverse problem in the wild. The framework is inspired by StyleGAN [19], GFPGAN [15], and GPEN [16], consisting of an asymmetric codec and StyleGAN2 prior network. Firstly, We input a low-quality image x into the codec, in which the encoder has one more MMRB layer in each scale than the decoder. That is because the encoder needs to provide more natural and reliable face latent features for the generator. The MMRB layer proposed by us can better extract the weak and few texture features in the degraded images. The input image x is then mapped to the closest latent codes Z in StyleGAN2 by the encoder. It can be seen from StyleGAN [19] and StyleGAN2 [20] that images can be generated only by latent codes without noise branches, but the generated results lack rich and real texture information. Aiming to balance the fidelity and authenticity of the restoration results, we use the decoder and skip connections to reconstruct the multi-scale downsampled features, and directly output the reconstructed features at each level to the noise branches in StyleGAN2. This process also benefits from the different practices of GFPGAN [15] and GPEN [16] networks. We have also verified the function of this process during training and have found that the reconstructed image has richer and more reasonable facial textures. Finally, to reduce the influence of degradation factors, we use L1 restoration loss similar to [15] for each resolution

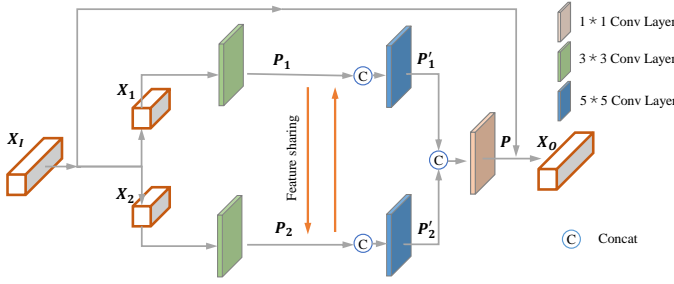


Fig. 3. Mixed Multi-path Residual block.

scale of the reconstructed image in the decoder. Finally, the process of codec is formulated by :

$$\hat{x}, Z = \text{Codec}(x), \quad (1)$$

Secondly, latent codes W , a learned constant feature tensor C and noise features \hat{x} are input into the pre-trained StyleGAN2, where W are latent codes decoupled by the latent codes Z through a mapping network of several multi-layer perceptron layers (MLP). feature space decoupling is formulated by:

$$W = \text{MLP}(Z), \quad (2)$$

The W ($w \in W$) are then broadcasted to each style block, in which the Mod and Demod indicate the modulation and demodulation operation of latent codes W , respectively. In particular, the input noise \hat{x} and the output \hat{y} of the style block after feature modulation are fused by concatenating rather than directly adding to convolutions in StyleGAN2, which enable introduces image features to be flexibly used for local texture restoration.

$$y_{i+1} = \text{Style}(w, y_i, \text{Concat}[\hat{x}_i, \hat{y}_i]). \quad (3)$$

The output feature map y will be input to the next style block. Based on the training method of joint fine-tuning, we can use style block to restore high-quality face images gradually from coarse to fine.

B. Mixed Multi-path Residual block

To extract slight and weak high-frequency textures in the degraded image, we propose a mixed multi-path residual block (MMRB). Here we will clearly describe its structure in Fig. 3. We design a two-branch and interactive feature extraction network, unlike previous works [34], [36], [46], [57]. We first equally split the input multi-channel feature maps X_I rather than reduce dimensionality using a 1×1 bottleneck layer.

$$X_1, X_2 = \text{Split}(X_I), \quad (4)$$

Where $\text{Split}(\cdot)$ represents the separation operation of the feature maps in the channel dimension. $X_I \in \mathbb{R}^{H \times W \times C}$. $X_1, X_2 \in \mathbb{R}^{H \times W \times C/2}$. We use then different convolution kernels to extract the features of the split feature maps. In order to improve the utilization of different scale features, skip connections are applied so that extracted features for different scales can be shared. The detailed definitions are as follows:

$$P_1 = F_1(X_1, W_1) = \sigma(W_1(X_1)), \quad (5)$$

$$P_2 = F_2(X_2, W_2) = \sigma(W_2(X_2)), \quad (6)$$

$$P'_1 = F_1(C_1, W_1) = \sigma(W_1(\text{Concat}[P_1, P_2])), \quad (7)$$

$$P'_2 = F_2(C_1, W_2) = \sigma(W_2(\text{Concat}[P_1, P_2])), \quad (8)$$

$$P = F_3(C_2, W_3) = \sigma(W_3(\text{Concat}[P'_1, P'_2])), \quad (9)$$

Where $F(\cdot, \cdot)$ represents convolution mapping functions. $\sigma(\cdot)$ stands for the PReLU nonlinear activation function [33]. W_1, W_2, W_3 indicate that the convolution kernel size used in the layer are 3, 5 and 1, respectively. $\text{Concat}[\cdot, \cdot]$ denotes the concatenation operation. Finally, through the dimensionality reduction of 1×1 bottleneck layer, the output feature parameters are significantly reduced.

In order to make the block more efficient and practical, we adopt residual learning similar to in ResNet [34] to each MMRB. Formally, we describe the MMRB layer as:

$$X_O = X_I + P. \quad (10)$$

Where X_O represents the MMRB's output. $P \in \mathbb{R}^{H \times W \times C}$ and is the output of multi-path feature maps fusion. In practice, The MMRB layer is applied to the encoder level by level from shallow layer to deep layer to improve our network's performance. What is more, it introduces fewer parameters and can be plug-and-play to enhance the ability of feature extraction in different models.

C. Freezing Discriminator

Thanks to the powerful generation ability of the StyleGAN2 [20] prior model, the generated face image is genuinely diversified in structure, texture, and color information. We use the StyleGAN2 model as a generative facial prior and adopt a jointly fine-tuning training strategy for the pre-trained StyleGAN2 and codec. Fine-tuning the pre-trained StyleGAN2 model can better fit the complex degraded multi-pose face data into the target distribution. While the source domain and target domain are the same in our work. To make the distribution generated results better consistent with the target distribution, we introduce a Freeze Discriminator (FreezeD) training skill [49] for the StyleGAN2 to better learn the target distribution by freezing the higher-resolution layer of the discriminator during the training process. We find that simply freezing the lower layers of the discriminator and only fine-tuning the upper layers performs surprisingly well, and the generator is more stable during training.

Where the pre-trained discriminator model comes from the training results published by [16], that is because it has a prior knowledge to distinguish high-quality images, and its target distribution for training is the same as ours. What's more, using the discriminator model and generator for joint fine-tuning can improve the quality of the overall image and speed up the training process.

D. Model Objectives

To jointly fine-tune our restoration model, we use the following loss functions: the adversarial loss, reconstruction loss, and identity preserving loss. The adversarial loss is composed of global adversarial loss and local adversarial loss, in which the global adversarial loss function is defined as

$$L_{adv-g} = \min_G \max_D \mathbb{E}_{(X)} \log \left(1 + \exp \left(-D \left(G \left(X' \right) \right) \right) \right) \quad (11)$$

Where X and X' denote the ground-truth image and the generated one, and G is the pre-trained StyleGAN2 for fine-tuning. D is the pre-trained discriminator from [16] and adopted the FreezeD strategy during training. The used logistic loss [31] is inherited from the StyleGAN2 prior network.

We believe StyleGAN2 [19] also incorporates geometric face priors for restoration. Therefore, we introduce local discriminators to focus generated results on local patch distributions, such as left eye, right eye, and mouth. By using local facial loss, we can effectively distinguish the high-frequency features of these regions to generate more natural and vivid local features. In particular, it can make our model better used to solve the unreal problem of multi-pose face image restoration in the wild.

We employ local discriminators for the left eye, right eye, and mouth for local facial loss. Firstly, the facial regions of interest (ROI) need to be cropped and aligned based on the 68 key points solved by the facial keypoint detection model [25] and Mask R-CNN [8]. For each region, We take adversarial training separately so that the local area of the restored image is more real and natural and closer to the distribution of the target data. The local facial loss is defined as follows:

$$L_{adv-l} = \sum_{ROI} \mathbb{E}_{(X'_{ROI})} \left[\log \left(1 - D_{ROI} \left(X'_{ROI} \right) \right) \right] \quad (12)$$

$$L_{adv} = \lambda_g L_{adv-g} + \lambda_l L_{adv-l} \quad (13)$$

Where the cross-entropy loss function is used and D_{ROI} is the local discriminator for each region. λ_g and λ_l represent the loss weights of global adversarial loss and local adversarial loss, respectively. We differentiate the weight of the discriminator to force the generator to focus on these facial regions during training. We adopt the L1-norm loss and feature matching loss as content loss L_C :

$$L_C = \lambda_{l1} \left\| X - X' \right\|_1 + \lambda_{FM} \mathbb{E} \left[\sum_{i=1}^N \left\| \psi_i(X) - \psi_i(X') \right\|_2 \right], \quad (14)$$

λ_{l1} and λ_{FM} represent the loss weights of the L1-norm loss and feature matching loss [55]. Inspired by [56], We give λ_{FM} a very small value of the weight parameter to avoid generating smooth results and causing checkerboard artifacts. ψ_i indicates the i -th Convolution layer of the pre-trained VGG network [53]. N is the total number of intermediate layers used for feature extraction. In order to enforce the restored face to have a small distance with the ground truth in the deep feature space, we introduce face preserving loss [32]:

$$L_{FP} = \lambda_{FP} \left\| \phi(X) - \phi(X') \right\|_1. \quad (15)$$

Where λ_{FP} denotes the loss weight. ϕ represents the face feature extractor that adopts the pre-trained face recognition ArcFace [47] model.

The overall loss optimization function used by our model objective is defined as

$$L_{total} = L_{adv} + L_C + L_{FP} \quad (16)$$

The loss hyper-parameters are set as follows: $\lambda_g = 0.5$, $\lambda_l = 3$, $\lambda_{l1} = 8$, $\lambda_{FM} = 0.02$, $\lambda_{FP} = 10$.

IV. EXPERIMENTS

A. Datasets

We train on the 70k high-quality face images from the FFHQ dataset, which is synthesized by [20]. We resize the resolution of all images to 512×512 during training. To make the training data more in line with the degradation of the real scene, We follow the practice in [18] [15] [16] and adopt the following degradation model with all possible degradation factors in the wild to synthesize LQ training data:

$$x = \mathbb{D}(y) = [(y \otimes k) \downarrow_s + n_\delta]_{JPEG_q} \quad (17)$$

\mathbb{D} denotes the degradation process for HQ images. The HQ face image y is first convolved \otimes with blur kernel k . Then, a downsampling operation with scale factor s is performed. The LQ image x is obtained by adding noise n . Finally, JPEG compression is also adopted and widely used in real-world images. To simulate the seriously degraded scene, we slightly increase the value of the degradation factor. We randomly sample k , s , δ and q from 41, [0.4 : 8], [0 : 25], [5 : 50] for each training pair in our experiments, respectively. In particular, we use Gaussian blur and motion blur to deal with the possible blur of the image in the natural scene.

Testing Datasets. To better verify the performance of our model on multi-pose face restoration in complex degraded scenes, we use various types of low-quality datasets for testing, and they do not overlap with the training data. We make a brief description of them respectively.

CelebA Data is a synthetic dataset with 30000 high-quality face images [54]. We select 2556 face images with complex facial posture and degrade the selected images using the above degradation model and parameters to verify the superiority of our algorithm.

LFW Data comes from [61] and is composed of more than 13000 face pictures of famous people all over the world with different orientations, expressions, and lighting environments. They are real low-quality images with only a single face. The image size is 250 pixels \times 250 pixels. We select 1610 images for testing.

FDDb Data comes from [63] and contains 5171 human faces in 2845 images taken from different natural scenes. The number of faces in the image is uncertain, not a single number. Moreover, the width and height of images are not equal, and the difference is noticeable. We select 1629 images for testing.

WebFace Data is collected face images from the Internet by [64], including tens of thousands of images with a size of 250 pixels \times 250 pixels. They are real low-quality images with only a single face and have also many old black-and-white photos. We select 804 images for testing.

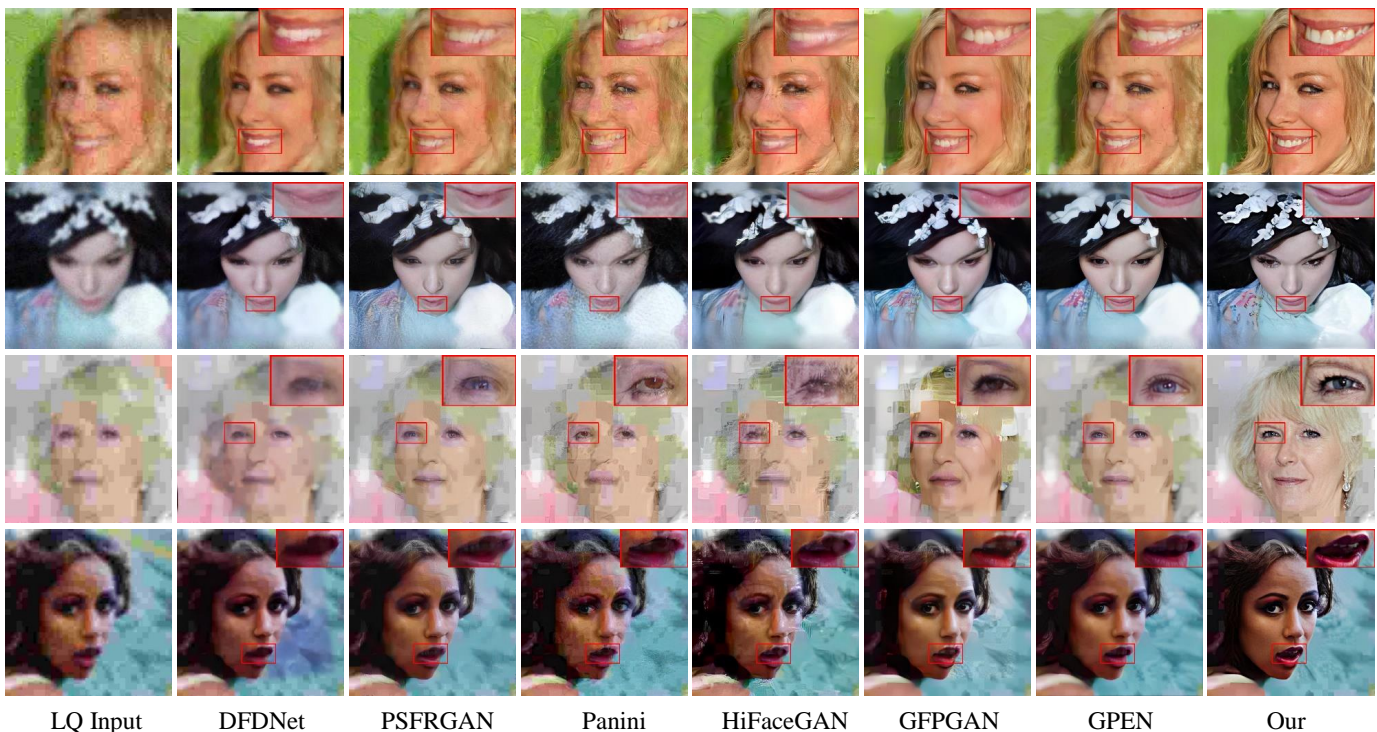


Fig. 4. Qualitative comparisons with several of the latest face restoration methods on the CelebA Data. To intuitively feel the performance difference of each algorithm, we enlarge and display the local area. **Zoom in for best view.**

B. Implementation Details and Evaluation Metrics

We adopt the FreezeD strategy [49] to the global discriminator from [16], and freeze the parameters of the first five convolution layers and fine-tune the remaining deep features. We then jointly fine-tune the Stylegan2 model retrained by [16] with the codec. The input image dimension mapped to the nearest latent codes is consistent with the pre-trained Stylegan2 model. At the same time, the resolution and dimension for the output feature maps of every level in the reconstruction process are consistent with the noise branch of the pre-trained model. For each MMRB layer, we use it layer by layer to extract weak texture features in low-quality images.

During the experiment, we train our model with Adam optimizer [65] and perform a total of 700k iterations with a batch size of 4. The learning rate (LR) varies for different parts, including the codec, the global discriminator, the local discriminator, the pre-trained Stylegan2 model, and noise branches. They are set to 2×10^{-3} , 2×10^{-5} , 2×10^{-3} , 2×10^{-4} and 2×10^{-3} , respectively. The local discriminator includes three facial components: left eye, right eye, and mouth. They use the same learning rate and model. Furthermore, a piece-wise attenuation strategy is adopted. We implement our models with the PyTorch framework and train them using two NVIDIA V100 GPUs.

For the evaluation, we employ a widely-used non-reference perceptual metric: NIQE [59]. Moreover, we also adopt pixel-wise metrics (PSNR and SSIM) and the perceptual metrics (LPIPS [60] and FID [58]) for the CelebA Data with Ground Truth (GT).

TABLE I
QUANTITATIVE COMPARISONS OF VARIOUS BFR METHODS ON CELEBA DATA. BOLD RED INDICATES THE BEST PERFORMANCE, AND BLUE INDICATES THE SECOND. REFERENCE IMAGE QUALITY EVALUATION METRICS ARE USED, SUCH AS PSNR, SSIM, LPIPS, AND FID, AND NON-REFERENCE IMAGE QUALITY PERCEPTUAL METRIC NIQE.

| Methods | PSNR \uparrow | SSIM \uparrow | LPIPS \downarrow | FID \downarrow | NIQE \downarrow |
|----------------|-----------------|-----------------|--------------------|------------------|-------------------|
| HiFaceGAN [12] | 24.506 | 0.612 | 0.196 | 31.545 | 4.427 |
| DFDNet [7] | 22.470 | 0.663 | 0.232 | 54.358 | 5.916 |
| PSFRGAN [5] | 24.884 | 0.663 | 0.192 | 34.695 | 4.765 |
| Panini [17] | 24.679 | 0.611 | 0.194 | 44.696 | 3.837 |
| GPEN [16] | 25.190 | 0.680 | 0.169 | 21.852 | 4.712 |
| GFPGAN [15] | 24.895 | 0.688 | 0.172 | 21.160 | 4.746 |
| Our | 26.034 | 0.702 | 0.162 | 16.080 | 4.285 |
| GT | ∞ | 1 | 0 | 2.478 | 4.188 |

C. Experiments on Synthetic Images

To better show the practicability and generality of our model, we verify the performance of face restoration and face super-resolution tasks based on the synthetic CelebA Data, respectively.

Face Restoration. To verify the superiority of the method mentioned in this paper, We make qualitative and quantitative comparisons with several of the latest blind face restoration methods, respectively, including DFDNet [7], PSFRGAN [5], Panini [17], HiFaceGAN [12], GFPGAN [15], and GPEN [16]. We introduce the index value corresponding to the Ground-Truth(GT) to understand better the difference between the test results of different methods and the GT in quantitative analyses.

The quantitative and qualitative results of different methods are shown in Tab. I and Fig. 4, respectively. Our method is optimal in all indicators and has the best performance

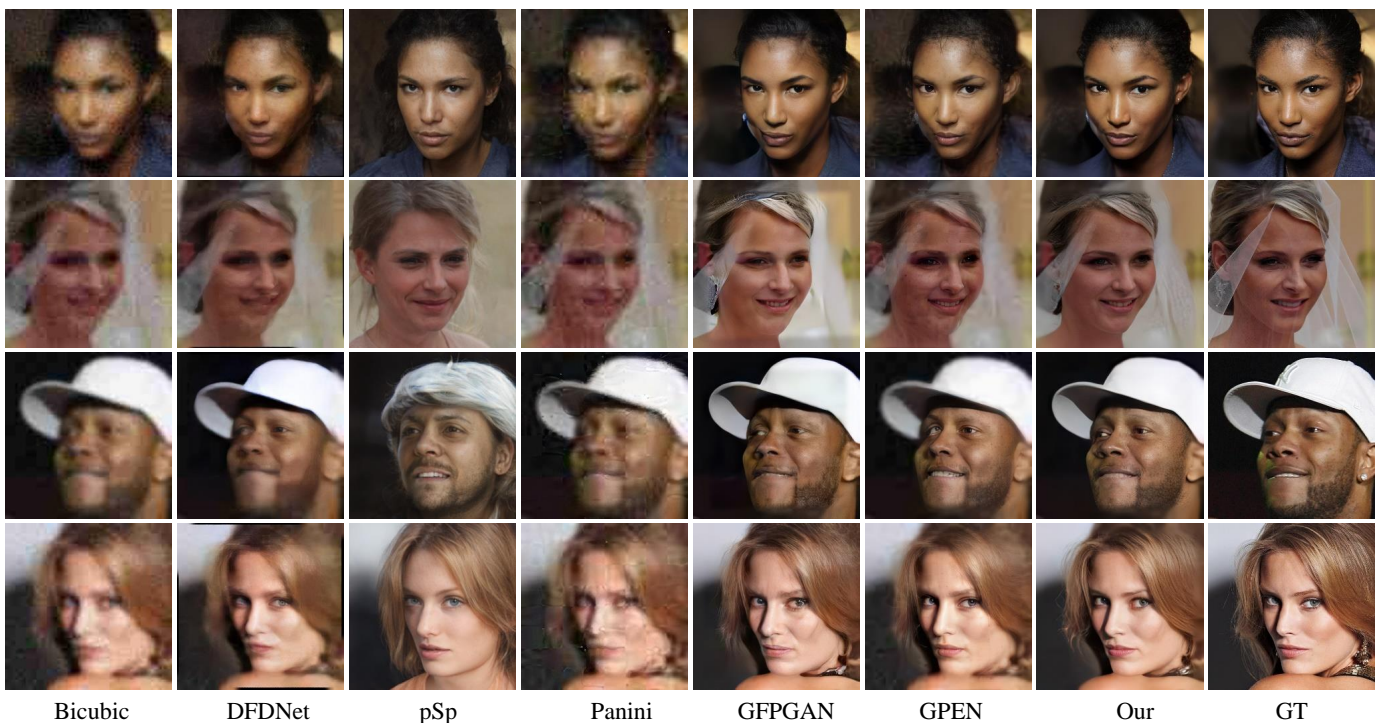


Fig. 5. Qualitative comparisons of 4x face super-resolution by different methods. We do not adopt local magnification displays for the qualitative comparison results, which intend to view the differences between them in the form of the whole picture. **Zoom in for best view.**

according to the quantitative results. Although the NIQE metric is slightly lower than the best, it does not affect the priority of our method. That is because this perceptual metric can only roughly reflect the difference between test images in deep space and the learned perceptual features and does not accurately represent the detailed effect of test images [66]. What’s more, thanks to the fine-tuning training strategy, the visual qualitative comparison results show that our method can flexibly restore the complex degraded multi-pose face image. The restoration results have the best visual sensory effect, especially in the eyes and mouth areas. The locally enlarged facial details show that the restored images are more realistic and natural, and the face details are more reasonable. In addition, it can be seen that our method can also improve the image quality of non-facial regions.

Face Super-resolution. We use the first 1500 images of CelebA Data and perform 4x downsampling of the input images to verify the super-resolution performance of different methods in the wild. Furthermore, we also make qualitative and quantitative comparisons with several state-of-the-art face super-resolution methods, including SuperFAN [4], pSp [13], Panini [17], HiFaceGAN [12], DFDNet [58], GFPGAN [15], and GPEN [16]. Our method needs to upsample the test data to the original scale and then input it into the network for testing.

The quantitative and qualitative results of different methods are shown in Tab. II and Fig. 5, respectively. As can be seen from the quantitative results, Our method can perform super-resolution on LQ images, and the output results are significantly better than other face super-resolution methods in all indicators. We do not adopt local magnification displays

TABLE II
QUANTITATIVE COMPARISONS OF VARIOUS FSR METHODS ON CELEBA DATA. WE USE THE BICUBIC INTERPOLATION METHOD FOR 4X DOWN-SAMPLING OF THE INPUT DATA TO VERIFY THE SUPER-RESOLUTION PERFORMANCE OF DIFFERENT METHODS. BOLD RED INDICATES THE BEST PERFORMANCE, AND BLUE INDICATES THE SECOND.

| Methods | PSNR \uparrow | SSIM \uparrow | LPIPS \downarrow | FID \downarrow | NIQE \downarrow |
|----------------|-----------------|-----------------|--------------------|------------------|-------------------|
| Bicubic | 23.757 | 0.641 | 0.297 | 148.468 | 10.460 |
| SuperFAN [4] | 23.193 | 0.617 | 0.290 | 152.188 | 7.857 |
| pSp [13] | 18.493 | 0.580 | 0.242 | 67.596 | 5.647 |
| HiFaceGAN [12] | 19.946 | 0.470 | 0.326 | 230.756 | 10.480 |
| DFDNet [58] | 21.772 | 0.638 | 0.260 | 93.107 | 6.416 |
| Panini [17] | 23.417 | 0.620 | 0.278 | 165.834 | 6.898 |
| GPEN [16] | 24.248 | 0.658 | 0.217 | 50.348 | 5.886 |
| GFPGAN [15] | 23.780 | 0.656 | 0.190 | 32.894 | 4.955 |
| Our | 24.797 | 0.674 | 0.189 | 27.403 | 4.449 |
| GT | ∞ | 1 | 0 | 2.413 | 4.036 |

for the qualitative comparison results, which intend to view the differences between them in the form of the whole picture. By visualizing the comparison results, our results are closer to the GT and have fewer or less noticeable artifacts and texture blur, whether in facial texture, hair, or background. Although the pSp method [13] also shows promising results in the visualization effect, it is quite different from the GT due to its design idea.

D. Experiments on Images in the Real-World

We evaluate our method on Fddb Data, LFW Data, and WedFace Data, which are face images with complex facial poses in real scenes and suffer from multiple complex unknown degradations. To test the generalization ability, We make qualitative and quantitative comparisons with several

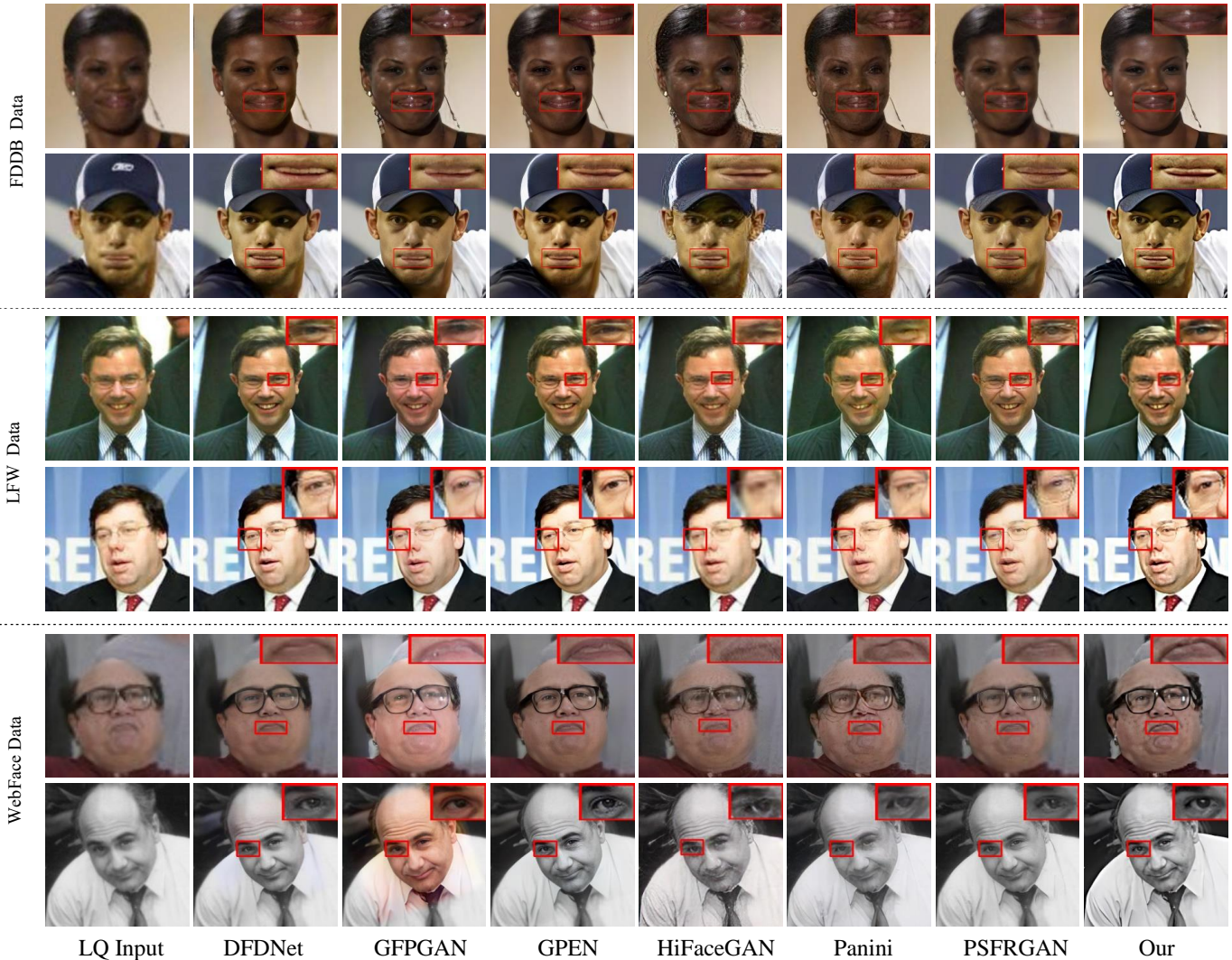


Fig. 6. Qualitative comparisons on Fddb Data, LFW Data, and WebFace Data. **Zoom in for best view.**

TABLE III
QUANTITATIVE COMPARISONS OF VARIOUS FSR METHODS IN THE WILD, SUCH AS **FDDB DATA**, **LFW DATA**, **WEBFACE DATA**. ONLY THE NON-REFERENCE EVALUATION MATRIX NIQE IS USED. “-” MEANS THAT THE RESULT IS NOT EXISTENT.

| Dataset Methods | FDDB Data NIQE ↓ | LFW Data NIQE ↓ | WebFace Data NIQE ↓ |
|-----------------|----------------------------|---------------------------|-------------------------------|
| Input | 4.262 | 5.454 | 4.875 |
| HiFaceGAN [12] | 3.956 | 4.548 | 4.969 |
| DFDNet [7] | 4.153 | 4.990 | 5.449 |
| PSFRGAN [5] | 4.334 | 5.461 | 5.830 |
| Panini [17] | - | 4.694 | 4.605 |
| GPEN [16] | 4.11 | 5.418 | 5.793 |
| GFPGAN [15] | 4.009 | 4.982 | 5.313 |
| Ours | 3.578 | 4.548 | 4.875 |

blind face restoration methods, such as DFDNet [7], PSFRGAN [5], Panini [17], HiFaceGAN [12], GFPGAN [15], and GPEN [16]. Since there is no GT in the real degraded image, we use the non-reference perceptual metric (NIQE) to test the performance of different methods. For Fddb data, in order to facilitate qualitative comparison, we select some images and

use the pre-trained RetinaFace face detection model [9] to cut out a single face with consistent width and height for testing.

The quantitative and qualitative results are presented in Tab. III and Fig. 6. It can be seen that our method still has prominent leadership in quantitative indicators and visualization results. Thanks to our careful design model and the excellent training strategy, the restored images have more apparent texture and higher quality, especially the local content is more realistic and reasonable. Although the numerical value is not the best on WebFace Data, it is evident from the visual effect that our method still has excellent performance. In the quantitative comparison, Panini method [17] lacks test results on Fddb Data, mainly because the images in the dataset have the problem of unequal width and height. What’s more, this method strictly requires equal width and height of the input images.

E. Ablation Studies

To better understand the roles of different components and training strategies in our method, we train them separately



Fig. 7. Comparative results of different variables in our model. **Zoom in for best view.**

TABLE IV

ABLATION STUDY RESULTS OF DIFFERENT VARIANTS ON CELEBA DATA.

| Components | PSNR \uparrow | SSIM \uparrow | LPIPS \downarrow | FID \downarrow | NIQE \downarrow |
|-------------------|-----------------|-----------------|--------------------|------------------|-------------------|
| a) w/o MMRB | 25.977 | 0.699 | 0.163 | 17.027 | 4.682 |
| b) w/o FreezeD | 26.016 | 0.701 | 0.164 | 17.812 | 4.868 |
| c) w/o LocalD | 26.010 | 0.697 | 0.163 | 16.908 | 4.614 |
| d) w/o ft+FreezeD | 25.704 | 0.692 | 0.171 | 19.543 | 4.546 |
| All (Our) | 26.034 | 0.702 | 0.162 | 16.080 | 4.285 |

and use qualitative and quantitative comparisons to test the performance. The relevant variables involved are as follows: without MMRB layers(w/o MMRB), without Local Discriminator(w/o LocalD), without the Freezing Discriminator(w/o FreezeD), without fine-tuning and Freezing Discriminator skills(w/o ft+FreezeD). As can be seen from the Fig. 7 and Tab. IV, we can find that:

MMRB layers. When we remove the MMRB layers in the encoder, we find that the texture information of the restored image is missing, and the authenticity is weakened, especially in local areas of the image.

Local Discriminator. In the training process, if the network lacks local discriminators and the constraint of local adversarial loss, the restoration results are not natural enough and complete, and the visual sense is poor. That is mainly because the eyes and mouth significantly impact the overall quality.

Fine-tuning and FreezeD strategies. The training strategies significantly impact the restoration results of our model, whether they are visualization results or evaluation metrics. Therefore, if the training strategies adopt complex degraded multi-pose face images, the weights of codec and GAN prior network can be adjusted jointly to fit the real high fidelity face images better. These strategies can also greatly reduce the distribution difference between the restoration result and the target domain.

FreezeD strategy. This component also significantly impacts the restoration of local texture and the overall image quality. Meanwhile, thanks to the discriminator model with rich prior knowledge, the adversarial loss can converge faster and more stable in the training process.

V. CONCLUSION

Aiming at the problem that complex degraded multi-pose and multi-expression face images are challenging to restore, we meticulously designed a network with a prior facial model for blind face restoration. To better fit the distribution model of diversified face images suitable for the natural scene and

improve the quality of the overall images, we fine-tune the pre-trained StyleGAN2 model and adopt the FreezeD strategy for the global discriminator network. Moreover, we apply MMRB layers to extract weak texture features in the input image. Because the facial eye and mouth regions are difficult to recover, We use different local adversarial losses to constrain the proposed model for these regions to restore the real face images. Extensive experiments on synthetic data and multiple real-world images demonstrate that our model can be used to restore complex degraded multi-pose face images. The restoration results have rich textures, natural details, and great visual sense, which reaches the latest Optimal blind face restoration methods.

Most importantly, our model can also improve the image quality of non-facial regions and might be applicable to restoring old photos and film and television works and achieving face super-resolution tasks in the wild.

REFERENCES

- [1] Z. Shen, W.-S. Lai, T. Xu, J. Kautz, and M.-H. Yang, "Deep semantic face deblurring," in *Proc. IEEE Conf. Comput. Vis. Pattern Recognit. (CVPR)*, 2018, pp. 8260–8269.
- [2] C. Dong, Y. Deng, C. C. Loy, and X. Tang, "Compression artifacts reduction by a deep convolutional network," in *Proc. IEEE Conf. Comput. Vis. Pattern Recognit. (CVPR)*, 2015, pp. 576–584.
- [3] X. Yu and F. Porikli, "Hallucinating very low-resolution unaligned and noisy face images by transformative discriminative autoencoders," in *Proc. IEEE Conf. Comput. Vis. Pattern Recognit. (CVPR)*, 2017, pp. 3760–3768.
- [4] A. Bulat and G. Tzimiropoulos, "Super-fan: Integrated facial landmark localization and super-resolution of real-world low resolution faces in arbitrary poses with gans," in *Proc. IEEE Conf. Comput. Vis. Pattern Recognit. (CVPR)*, 2018, pp. 109–117.
- [5] C. Chen, X. Li, L. Yang, X. Lin, L. Zhang, and K.-Y. K. Wong, "Progressive semantic-aware style transformation for blind face restoration," in *Proc. IEEE Conf. Comput. Vis. Pattern Recognit. (CVPR)*, 2021, pp. 11 896–11 905.
- [6] J. He, W. Shi, K. Chen, L. Fu, and C. Dong, "Gcfsr: a generative and controllable face super resolution method without facial and gan priors," 2022, *arXiv:2203.07319*. [Online]. Available: <https://arxiv.org/abs/2203.07319>.
- [7] X. Li, C. Chen, S. Zhou, X. Lin, W. Zuo, and L. Zhang, "Blind face restoration via deep multi-scale component dictionaries," in *Proc. Comput. Vis. (ECCV)*. Springer, 2020, pp. 399–415.
- [8] K. He, G. Gkioxari, P. Dollár, and R. Girshick, "Mask r-cnn," in *Proc. IEEE Conf. Comput. Vis. Pattern Recognit. (CVPR)*, 2017, pp. 2961–2969.
- [9] J. Deng, J. Guo, E. Ververas, I. Kotsia, and S. Zafeiriou, "Retinaface: Single-shot multi-level face localisation in the wild," in *Proc. IEEE Conf. Comput. Vis. Pattern Recognit. (CVPR)*, 2020, pp. 5203–5212.
- [10] J. Gu, Y. Shen, and B. Zhou, "Image processing using multi-code gan prior," in *Proc. IEEE Conf. Comput. Vis. Pattern Recognit. (CVPR)*, 2020, pp. 3012–3021.
- [11] S. Menon, A. Damian, S. Hu, N. Ravi, and C. Rudin, "Pulse: Self-supervised photo upsampling via latent space exploration of generative models," in *Proc. IEEE Conf. Comput. Vis. Pattern Recognit. (CVPR)*, 2020, pp. 2437–2445.
- [12] L. Yang, S. Wang, S. Ma, W. Gao, C. Liu, P. Wang, and P. Ren, "Hifacegan: Face renovation via collaborative suppression and replenishment," in *Proc. ACM Multimedia Conf. (MM)*, 2020, pp. 1551–1560.
- [13] E. Richardson, Y. Alaluf, O. Patashnik, Y. Nitzan, Y. Azar, S. Shapiro, and D. Cohen-Or, "Encoding in style: a stylegan encoder for image-to-image translation," in *Proc. IEEE Conf. Comput. Vis. Pattern Recognit. (CVPR)*, 2021, pp. 2287–2296.
- [14] Z. Cheng, X. Zhu, and S. Gong, "Characteristic regularisation for super-resolving face images," in *Proc. IEEE Conf. Comput. Vis. Pattern Recognit. (CVPR)*, 2020, pp. 2435–2444.
- [15] X. Wang, Y. Li, H. Zhang, and Y. Shan, "Towards real-world blind face restoration with generative facial prior," in *Proc. IEEE Conf. Comput. Vis. Pattern Recognit. (CVPR)*, 2021, pp. 9168–9178.

- [16] T. Yang, P. Ren, X. Xie, and L. Zhang, "Gan prior embedded network for blind face restoration in the wild," in *Proc. IEEE Conf. Comput. Vis. Pattern Recognit. (CVPR)*, 2021, pp. 672–681.
- [17] Y. Wang, Y. Hu, and J. Zhang, "Panini-net: Gan prior based degradation-aware feature interpolation for face restoration," 2022, *arXiv:2203.08444*. [Online]. Available: <https://arxiv.org/abs/2203.08444>.
- [18] X. Wang, L. Xie, C. Dong, and Y. Shan, "Real-esrgan: Training real-world blind super-resolution with pure synthetic data," in *Proc. IEEE Conf. Comput. Vis. Pattern Recognit. (CVPR)*, 2021, pp. 1905–1914.
- [19] T. Karras, S. Laine, and T. Aila, "A style-based generator architecture for generative adversarial networks," in *Proc. IEEE Conf. Comput. Vis. Pattern Recognit. (CVPR)*, 2019, pp. 4401–4410.
- [20] T. Karras, S. Laine, M. Aittala, J. Hellsten, J. Lehtinen, and T. Aila, "Analyzing and improving the image quality of stylegan," in *Proc. IEEE Conf. Comput. Vis. Pattern Recognit. (CVPR)*, 2020, pp. 8110–8119.
- [21] T. Karras, M. Aittala, S. Laine, E. Härkönen, J. Hellsten, J. Lehtinen, and T. Aila, "Alias-free generative adversarial networks," *Proc. Adv. Neural Inf. Process. Syst. (NeurIPS)*, vol. 34, 2021.
- [22] Y. Chen, Y. Tai, X. Liu, C. Shen, and J. Yang, "Fsrnet: End-to-end learning face super-resolution with facial priors," in *Proc. IEEE Conf. Comput. Vis. Pattern Recognit. (CVPR)*, 2018, pp. 2492–2501.
- [23] Z. Wang, J. Chen, and S. C. Hoi, "Deep learning for image super-resolution: A survey," *IEEE Trans. Pattern Anal. Machine Intell.*, vol. 43, no. 10, pp. 3365–3387, 2020.
- [24] J. Jiang, C. Wang, X. Liu, and J. Ma, "Deep learning-based face super-resolution: A survey," *ACM Comput. Surv.*, vol. 55, no. 1, pp. 1–36, 2021.
- [25] H. Jin, S. Liao, and L. Shao, "Pixel-in-pixel net: Towards efficient facial landmark detection in the wild," *Int. J. Comput. Vis.*, vol. 129, no. 12, pp. 3174–3194, 2021.
- [26] S. Sharma and V. Kumar, "3d landmark-based face restoration for recognition using variational autoencoder and triplet loss," *IET Biom.*, vol. 10, no. 1, pp. 87–98, 2021.
- [27] O. Tuzel, Y. Taguchi, and J. R. Hershey, "Global-local face up-sampling network," 2016, *arXiv:1603.07235*. [Online]. Available: <https://arxiv.org/abs/1603.07235>.
- [28] K. Jiang, Z. Wang, P. Yi, T. Lu, J. Jiang, and Z. Xiong, "Dual-path deep fusion network for face image hallucination," *IEEE Trans. Neural Networks Learn. Syst.*, 2020.
- [29] E. Zhou, H. Fan, Z. Cao, Y. Jiang, and Q. Yin, "Learning face hallucination in the wild," in *Proc. AAAI Conf. Artif. Intell. (AAAI)*, 2015.
- [30] M. Zhang and Q. Ling, "Supervised pixel-wise gan for face super-resolution," *IEEE Trans. Multimedia*, vol. 23, pp. 1938–1950, 2020.
- [31] I. Goodfellow, J. Pouget-Abadie, M. Mirza, B. Xu, D. Warde-Farley, S. Ozair, A. Courville, and Y. Bengio, "Generative adversarial nets," *Proc. Adv. Neural Inf. Process. Syst. (NeurIPS)*, vol. 27, 2014.
- [32] R. Huang, S. Zhang, T. Li, and R. He, "Beyond face rotation: Global and local perception gan for photorealistic and identity preserving frontal view synthesis," in *Proc. IEEE Int. Conf. Comput. Vis. (ICCV)*, 2017, pp. 2439–2448.
- [33] K. He, X. Zhang, S. Ren, and J. Sun, "Delving deep into rectifiers: Surpassing human-level performance on imagenet classification," in *Proc. IEEE Int. Conf. Comput. Vis. (ICCV)*, 2015, pp. 1026–1034.
- [34] Y. Zhang, Y. Tian, Y. Kong, B. Zhong, and Y. Fu, "Residual dense network for image super-resolution," in *Proc. IEEE Conf. Comput. Vis. Pattern Recognit. (CVPR)*, 2018, pp. 2472–2481.
- [35] K. He, X. Zhang, S. Ren, and J. Sun, "Deep residual learning for image recognition," in *Proc. IEEE Conf. Comput. Vis. Pattern Recognit. (CVPR)*, 2016, pp. 770–778.
- [36] C. Szegedy, W. Liu, Y. Jia, P. Sermanet, S. Reed, D. Anguelov, D. Erhan, V. Vanhoucke, and A. Rabinovich, "Going deeper with convolutions," in *Proc. IEEE Conf. Comput. Vis. Pattern Recognit. (CVPR)*, 2015, pp. 1–9.
- [37] G. Song, L. Luo, J. Liu, W.-C. Ma, C. Lai, C. Zheng, and T.-J. Cham, "Agilegan: stylizing portraits by inversion-consistent transfer learning," *ACM Trans. Graph.*, vol. 40, no. 4, pp. 1–13, 2021.
- [38] O. Tov, Y. Alaluf, Y. Nitzan, O. Patashnik, and D. Cohen-Or, "Designing an encoder for stylegan image manipulation," *ACM Trans. Graph.*, vol. 40, no. 4, pp. 1–14, 2021.
- [39] P. Zhu, R. Abdal, J. Femiani, and P. Wonka, "Mind the gap: Domain gap control for single shot domain adaptation for generative adversarial networks," 2021, *arXiv:2110.08398*. [Online]. Available: <https://arxiv.org/abs/2110.08398>.
- [40] J. Huang, J. Liao, and S. Kwong, "Unsupervised image-to-image translation via pre-trained stylegan2 network," *IEEE Trans. Multimedia*, vol. 24, pp. 1435–1448, 2021.
- [41] W. Zhuang, X. Gan, Y. Wen, X. Zhang, S. Zhang, and S. Yi, "Towards unsupervised domain adaptation for deep face recognition under privacy constraints via federated learning," 2021, *arXiv:2105.07606*. [Online]. Available: <https://arxiv.org/abs/2105.07606>.
- [42] R. Liu, Y. Ge, C. L. Choi, X. Wang, and H. Li, "Divco: Diverse conditional image synthesis via contrastive generative adversarial network," in *Proc. IEEE Conf. Comput. Vis. Pattern Recognit. (CVPR)*, 2021, pp. 16 377–16 386.
- [43] T. Park, M.-Y. Liu, T.-C. Wang, and J.-Y. Zhu, "Semantic image synthesis with spatially-adaptive normalization," in *Proc. IEEE Conf. Comput. Vis. Pattern Recognit. (CVPR)*, 2019, pp. 2337–2346.
- [44] A. Akerberg, K. Nasrollahi, and T. B. Moeslund, "Real-world super-resolution of face-images from surveillance cameras," *IET Image Process.*, vol. 16, no. 2, pp. 442–452, 2022.
- [45] C. Chen, D. Gong, H. Wang, Z. Li, and K.-Y. K. Wong, "Learning spatial attention for face super-resolution," *IEEE Trans. Image Process.*, vol. 30, pp. 1219–1231, 2020.
- [46] J. Li, F. Fang, K. Mei, and G. Zhang, "Multi-scale residual network for image super-resolution," in *Proc. Eur. Conf. Comput. Vis. (ECCV)*, 2018, pp. 517–532.
- [47] D. Jiankang, G. Jia, Z. Yuxiang, Y. Jinke, K. Irene, and Z. Stefanos, "Retinaface: Single-stage dense face localisation in the wild," 2019, *arXiv:1905.00641*. [Online]. Available: <https://arxiv.org/abs/1905.00641>.
- [48] J. Back, "Fine-tuning stylegan2 for cartoon face generation," 2021, *arXiv:2106.12445*. [Online]. Available: <https://arxiv.org/abs/2106.12445>.
- [49] S. Mo, M. Cho, and J. Shin, "Freeze the discriminator: a simple baseline for fine-tuning gans," 2020, *arXiv:2002.10964*. [Online]. Available: <https://arxiv.org/abs/2002.10964>.
- [50] C. Zhang and Q. Zhao, "Deep discriminative domain adaptation," *Inf. Sci.*, vol. 575, pp. 599–610, 2021.
- [51] K. Zhou, Z. Liu, Y. Qiao, T. Xiang, and C. C. Loy, "Domain generalization in vision: A survey," 2021, *arXiv:2103.02503*. [Online]. Available: <https://arxiv.org/abs/2103.02503>.
- [52] T. Karras, M. Aittala, J. Hellsten, S. Laine, J. Lehtinen, and T. Aila, "Training generative adversarial networks with limited data," *Proc. Adv. Neural Inf. Process. Syst. (NeurIPS)*, vol. 33, pp. 12 104–12 114, 2020.
- [53] K. Simonyan and A. Zisserman, "Very deep convolutional networks for large-scale image recognition," 2014, *arXiv:1409.1556*. [Online]. Available: <https://arxiv.org/abs/1409.1556>.
- [54] Z. Liu, P. Luo, X. Wang, and X. Tang, "Deep learning face attributes in the wild," in *Proc. IEEE Int. Conf. Comput. Vis. (ICCV)*, 2015, pp. 3730–3738.
- [55] T.-C. Wang, M.-Y. Liu, J.-Y. Zhu, A. Tao, J. Kautz, and B. Catanzaro, "High-resolution image synthesis and semantic manipulation with conditional gans," in *Proc. IEEE Conf. Comput. Vis. Pattern Recognit. (CVPR)*, 2018, pp. 8798–8807.
- [56] H. Zhao, O. Gallo, I. Frosio, and J. Kautz, "Loss functions for image restoration with neural networks," *IEEE Trans. Comput. Imaging*, vol. 3, no. 1, pp. 47–57, 2016.
- [57] C. Szegedy, S. Ioffe, V. Vanhoucke, and A. A. Alemi, "Inception-v4, inception-resnet and the impact of residual connections on learning," in *Proc. AAAI Conf. Artif. Intell. (AAAI)*, 2017.
- [58] M. Heusel, H. Ramsauer, T. Unterthiner, B. Nessler, and S. Hochreiter, "Gans trained by a two time-scale update rule converge to a local nash equilibrium," *Proc. Adv. Neural Inf. Process. Syst. (NeurIPS)*, vol. 30, 2017.
- [59] A. Mittal, R. Soundararajan, and A. C. Bovik, "Making a "completely blind" image quality analyzer," *IEEE Signal Process. Lett.*, vol. 20, no. 3, pp. 209–212, 2012.
- [60] R. Zhang, P. Isola, A. A. Efros, E. Shechtman, and O. Wang, "The unreasonable effectiveness of deep features as a perceptual metric," in *Proc. IEEE Conf. Comput. Vis. Pattern Recognit. (CVPR)*, 2018, pp. 586–595.
- [61] G. B. Huang, M. Mattar, T. Berg, and E. Learned-Miller, "Labeled faces in the wild: A database for studying face recognition in unconstrained environments," in *Workshop on faces in 'Real-Life' Images: detection, alignment, and recognition*, 2008.
- [62] X. Li, M. Liu, Y. Ye, W. Zuo, L. Lin, and R. Yang, "Learning warped guidance for blind face restoration," in *Proc. Eur. Conf. Comput. Vis. (ECCV)*, 2018, pp. 272–289.

- [63] V. Jain and E. Learned-Miller, "Fddb: A benchmark for face detection in unconstrained settings," University of Massachusetts, Amherst, Tech. Rep. UM-CS-2010-009, 2010.
- [64] D. Yi, Z. Lei, S. Liao, and S. Z. Li, "Learning face representation from scratch," 2014, *arXiv:1411.7923*. [Online]. Available: <https://arxiv.org/abs/1411.7923>.
- [65] D. P. Kingma and J. Ba, "Adam: A method for stochastic optimization," 2014, *arXiv:1412.6980*. [Online]. Available: <https://arxiv.org/abs/1412.6980>.
- [66] Y. Blau, R. Mechrez, R. Timofte, T. Michaeli, and L. Zelnik-Manor, "The 2018 pirm challenge on perceptual image super-resolution," in *Proc. Eur. Conf. Comput. Vis. Workshops (ECCVW)*, 2018, pp. 0–0.



Kai Hu received the B.S. degree in optoelectronic information science and engineering from North University of China, Taiyuan, in 2017, and the M.S. degree in electronic and communication engineering from Tianjin University, Tianjin, in 2021, where he is currently pursuing the Ph.D. degree. His research interests include image/video processing and computer vision.



Gang Yu is a research leader at Tencent. He received Ph.D. from Nanyang Technological University (NTU), Singapore. Before joining Tencent, he was the team leader in Megvii, leading the development of detection/segmentation techniques for mobile and embedded devices. He has published more than 30 papers in top journals and conferences. He is the winner for more than ten challenges, including COCO detection/skeleton (2017 & 2018), Widerface Face Detection (2018), ActivityNet AVA Detection (2018), and WAD Instance Segmentation (2018). He received Microsoft Research Asia Fellowship in 2011.



Bin Fu is a director at Tencent. He leads the development and research team for GY-Lab. His research results have been widely used in Tencent products like QQ.



Yu Liu (M'06) received his BEng in electronic engineering from Tianjin University, Tianjin, China, in 1998. From 1998 to 2000, he worked as an electronic engineer in Shenzhen, China. In 2000, he returned to Tianjin University and received his MEng in information and communication engineering and Ph.D. in signal and information processing both from Tianjin University in 2002 and 2005, respectively. Currently, he is a full professor with the School of Microelectronics, Tianjin University. From 2011 to 2012, Dr. Liu was a visiting research fellow with the Department of Electrical Engineering, Princeton University, Princeton, NJ, USA. His research interests include sensing and applications in multimedia signal processing, compressed sensing, and machine intelligence.



Renhe Liu received his B.S. degree in communication engineering from Guangxi University, Nanning, China, in 2016, and he is currently working towards a Ph.D. degree at the School of Microelectronic, Tianjin University, Tianjin, China. His research interests include multimedia signal and image processing.



Wei Lu received his B.Eng. degree in Electronic Engineering, and Ph.D. degree in signal and information processing from Tianjin University, Tianjin, China, in 1998 and 2003 respectively. He is currently an associate professor in the School of Electrical Engineering, Tianjin University. His teaching and research interests include digital image processing, pattern recognition and embedded systems.